Dispersion compensation in an open-loop all-optical chaotic communication system*

Liu Hui-Jie(刘慧杰)[a)b)†], Ren Bin(任 斌)[b)], and Feng Jiu-Chao(冯久超)[a)]

[a)] *School of Electronic and Information Engineering, South China University of Technology, Guangzhou* 510641, *China*
[b)] *Department of Electronic Engineering, Dongguan University of Technology, Dongguan* 523808, *China*

(Received 29 August 2011; revised manuscript received 24 October 2011)

The optical chaotic communication system using open-loop fiber transmission is studied under strong injection conditions. The optical chaotic communication system with open-loop configuration is studied using fiber transmission under strong injection conditions. The performances of fiber links composed of two types of fiber segments in different dispersion compensation maps are compared by testing the quality of the recovered message with different bit rates and encrypted by chaotic modulation (CM) or chaotic shift keying (CSK). The result indicates that the performance of the pre-compensation map is always worst. Two types of symmetrical maps are identical whatever the encryption method and bit-rate of message are. For the transmitting and the recovering of message of lower bit rate (1 Gb/s), the post-compensation map is the best scheme. However, for the message of higher bit rate (2.5 Gb/s), the parameters in communication system need to be modified properly in order to adapt to the high-speed application. Meanwhile, two types of symmetrical maps are the best scheme. In addition, the CM method is superior to the CSK method for high-speed applications. It is in accordance with the result in a back-to-back configuration system.

Keywords: chaotic communication, dispersion compensation, semiconductor lasers, strong injection, open-loop configuration

PACS: 05.45.–a, 05.45.Pq, 05.45.Vx **DOI:** 10.1088/1674-1056/21/4/040501

1. Introduction

Owing to the high dimensionality, wide bandwidth and low attenuation, the optical chaos communication system has potential applications in remote and high-speed areas. The chaos phenomenon and chaotic synchronization have been found in several systems, such as semiconductor lasers,[1−7] solid state lasers,[8,9] gas lasers,[10,11] and so on. The chaotic secure communication using semiconductor lasers (SLs) has been studied intensively in recent years. Optical feedback, optoelectronic feedback, and optical injection are common methods to make SLs operate in the chaotic regime. Two categories of optical chaos communication systems based on external optical feedback have been developed, i.e. closed-loop and open-loop schemes. Although the closed-loop scheme is studied more than the open-loop scheme, it is not suitable for practical application because of the strict requirement for parameter matching.[12−15] For the open-loop case, there are two types of applications, weak injection and strong injection. Under the condition of weak injection, the injection strength in the receiver must be equal to the feedback strength in the transmitter to achieve identical synchronization. However, isochronous synchronization can be achieved for a wide parameter detuning between transmitter and receiver. For the case of an open-loop scheme, most of investigations focus on the synchronization of the system in back-to-back configuration where the transmission link is neglected. A few researchers have considered the fiber link in their research.[2,16,17] The system discussed in Ref. [2] is in closed-loop configuration. And only two kinds of dispersion compensation maps are compared by numerical investigation. Meanwhile, different results are achieved on encryption methods in fiber transmission system research compared with that of the back-to-back configuration system. The transmitter and the receiver in Refs. [16] and [17] were subjected to external injection. Moreover, the influence of the fiber link on performance was not considered. Thus, further research on a remote optical feedback chaotic communication system

*Project supported by the National Natural Science Foundation of China (Grant No. 60872123), the Joint Fund of the National Natural Science Foundation and the Guangdong Provincial Natural Science Foundation, China (Grant No. U0835001), and the Guangdong Provincial Natural Science Foundation (Grant No. S2011010002144).

†Corresponding author. E-mail: Liuhj@dgut.edu.cn

© 2012 Chinese Physical Society and IOP Publishing Ltd

using fiber transmission is necessary.

In this paper, we focus on the optical chaotic communication system in an open-loop configuration. The fiber link is composed of two types of fibers with four kinds of dispersion compensation maps, including two maps in Ref. [2] and other two new maps. The performances of the four maps are compared by testing the quality of the recovered message at different bit rates and encrypted by chaotic modulation (CM) or chaotic shift keying (CSK).

2. Theory and model

The block-diagram of the optical communication system used in our numerical simulation is shown in Fig.1. It consists of two identical Fabry–Perot semiconductor laser diodes respectively in the transmitter laser (TL) and the receiver laser (RL). Here, the communication system is configured in an open-loop scheme.

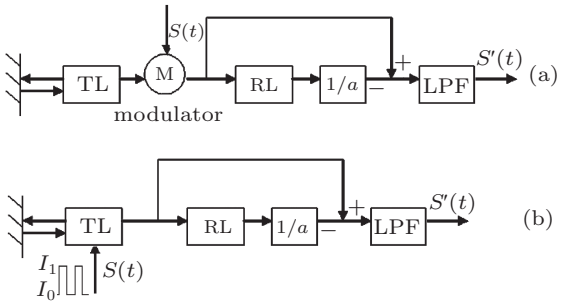


Fig. 1. Optical chaos communication system.

The dynamic behaviours of the two lasers can be described by the well-known Lang–Kobayashi equations, rewritten as follows:[1−5,18−23]

$$\frac{\mathrm{d}E_{\mathrm{t,r}}(t)}{\mathrm{d}t} = \frac{1-\mathrm{i}\,\alpha}{2}\left(G_{\mathrm{t,r}}(t)-\frac{1}{\tau_{p_{\mathrm{t,r}}}}\right)E_{\mathrm{t,r}}(t) + \gamma E_{\mathrm{t}}(t-T)\exp(\mathrm{i}\,\omega_0 T)+k_{\mathrm{inj}}E_{\mathrm{inj}}(t), \quad (1)$$

$$\frac{\mathrm{d}N_{\mathrm{t,r}}(t)}{\mathrm{d}t} = \frac{I_{\mathrm{b}}}{e}-\frac{N_{\mathrm{t,r}}(t)}{\tau_{n_{\mathrm{t,r}}}}-G_{\mathrm{t,r}}(t)\left|E_{\mathrm{t,r}}(t)\right|^2, \quad (2)$$

$$G_{\mathrm{t,r}}(t) = \frac{g(N_{\mathrm{t,r}}(t)-N_0)}{\left(1+s\left|E_{\mathrm{t,r}}\right|^2\right)}, \quad (3)$$

where the subscripts t and r refer to the TL and RL; $E_{\mathrm{t,r}}(t)$ is the complex slowly varying amplitude of the electric field; $N_{\mathrm{t,r}}(t)$ is the carrier number within the cavity; $G_{\mathrm{t,r}}(t)$ is the optical gain; $\omega_0(t)$ is the oscillation frequency of the TL and RL; γ is the feedback coefficient of TL which is subjected to external optical feedback; k_{inj} is the injection parameter; $E_{\mathrm{inj}}(t)$ is the optical field injected in RL. The second item in Eq. (1) corresponds to the TL, and the feedback term is valid only for the TL in the open-loop case. For back-to-back configuration, $E_{\mathrm{inj}}(t)=E_{\mathrm{t}}(t)$. However, for the fiber propagation link, $E_{\mathrm{inj}}(t)$ is the optical output after fiber. The injection term is valid only for the RL. The other parameters may be found in Table 1.

Rewrite $E_{\mathrm{t,r}}(t)$ as $E_{\mathrm{t,r}}(t)=A_{\mathrm{t,r}}(t)\exp(-\mathrm{i}\,\phi_{\mathrm{t,r}}(t))$, and $A_{\mathrm{t,r}}(t)=\sqrt{I_{\mathrm{t,r}}(t)}$. Here, $A_{\mathrm{t,r}}(t)$ and $\phi_{\mathrm{t,r}}(t))$ are the amplitude and phase of optical field respectively, $I_{\mathrm{t,r}}(t)$ is the intensity. According to these definitions, with considering the spontaneous emission process, equations (1)–(3) will be converted into

$$\begin{aligned}\frac{\mathrm{d}I_{\mathrm{t,r}}(t)}{\mathrm{d}t} &= \left(G_{\mathrm{t,r}}(t)-\frac{1}{\tau_{p_{\mathrm{t,r}}}}\right)I_{\mathrm{t,r}}(t)\\ &+2\gamma\sqrt{I_{\mathrm{t}}(t)I_{\mathrm{t}}(t-T)}\cos(\theta_{\mathrm{t}}(t))\\ &+2k_{\mathrm{inj}}\sqrt{I_{\mathrm{inj}}(t)I_r(t)}\cos(\theta_r(t))\\ &+\beta_{sp}N_{\mathrm{t,r}}(t)+F_{I_{\mathrm{t,r}}}(t), \quad (4)\\ \frac{\mathrm{d}\phi_{\mathrm{t,r}}(t)}{\mathrm{d}t} &= \frac{\alpha}{2}\left(G_{\mathrm{t,r}}(t)-\frac{1}{\tau_{p_{\mathrm{t,r}}}}\right)\\ &-\gamma\sqrt{\frac{I_{\mathrm{t}}(t-T)}{I_{\mathrm{t}}(t)}}\sin(\theta_{\mathrm{t}}(t))\\ &-k_{\mathrm{inj}}\sqrt{\frac{I_{\mathrm{inj}}(t)}{I_r(t)}}\sin(\theta_r(t))+F_{\phi_{\mathrm{t,r}}}(t), \quad (5)\\ \frac{\mathrm{d}N_{\mathrm{t,r}}(t)}{\mathrm{d}t} &= \frac{I_{\mathrm{b}}}{e}-\frac{N_{\mathrm{t,r}}(t)}{\tau_{n_{\mathrm{t,r}}}}-G_{\mathrm{t,r}}(t)\left|E_{\mathrm{t,r}}(t)\right|^2, \quad (6)\\ G_{\mathrm{t,r}}(t) &= \frac{g_(N_{\mathrm{t,r}}(t)-N_0)}{(1+sI_{\mathrm{t,r}}(t))}, \quad (7)\end{aligned}$$

where the noise terms are as follows:

$$F_{I_{\mathrm{t,r}}}(t)=\sqrt{\frac{2I_{\mathrm{t,r}}(t_i)\beta_{\mathrm{sp}}N_{\mathrm{t,r}}(t)}{\Delta t}}x_I, \quad (8)$$

$$F_{\phi_{\mathrm{t,r}}}(t)=\frac{1}{I_{\mathrm{t,r}}(t)}\sqrt{\frac{I_{\mathrm{t,r}}(t_i)\beta_{\mathrm{sp}}N_{\mathrm{t,r}}(t)}{2\Delta t}}x_\phi, \quad (9)$$

where x_I and x_ϕ are rand numbers with zero mean value and one variance. $\theta_{\mathrm{t}}(t)=\phi_{\mathrm{t}}(t)-\phi_{\mathrm{t}}(t-T)+\omega_0 T$, $\theta_{\mathrm{r}}(t)=\phi_{\mathrm{r}}(t)-\phi_{\mathrm{inj}}(t)$, $t_i=t-\Delta t$.

In Fig. 1, $S(t)$ is the encrypted message, and it comes from a pseudorandom bit sequence. However, $S(t)=1$ (or -1) for "1" bit (or "0" bit). In our analysis, two encryption methods are considered: CM [Fig. 1(a)] and CSK [Fig. 1(b)]. For the CM method, the encrypted message $S(t)$ modulates the chaotic carrier of the TL using an external modulator. The modulated wave can be described by $|E_{\mathrm{mod}}(t)|=(1+mS(t))\,|E_{\mathrm{t}}(t)|$ and propagated by fiber. The output of fiber is injected to the RL. Here,

m is the modulation depth. For the CSK method, $S(t)$ modulates the driving current of the TL according to the expression $I_{\rm b_t} = I_{\rm b}(1 + mS(t))$, while the driving current of the RL is fixed to be $I_{\rm b_r} = I_{\rm b}$.

For the application in the strong injection condition, we add the part $1/a$, where a is the gain of the system. By subtracting the adjusted output of RL from the output of TL (the output of fiber when fiber is used to propagate light signal), the encrypted information will be decoded and recovered. It has been proved that the adjusted decoding method can improve the quality of recovered information.

The performance of the system is numerically evaluated by the Q factor defined as follows:

$$Q = \frac{\langle X_1\rangle - \langle X_0\rangle}{\sigma_1 + \sigma_0}, \tag{10}$$

where $\langle X_1\rangle$ and $\langle X_0\rangle$ are the average optical powers of the bits in recovered information $S'(t)$ corresponding to "1" bits and "0" bits in $S(t)$; σ_1 and σ_0 are their standard deviations.

The light propagation along the fiber connecting the TL and the RL can be described by well-known generalized nonlinear Schrödinger equation

$$j\frac{\partial E}{\partial z} = -\frac{j}{2}\alpha E - \gamma |E|^2 E + \frac{1}{2}\beta_2\frac{\partial^2 E}{\partial t^2} + \frac{j}{6}\beta_3\frac{\partial^3 E}{\partial t^3}, \tag{11}$$

where E is the total field envelope, α is the fiber attenuation coefficient, γ is the nonlinear coefficient of the fiber responsible for self-phase modulation (SPM), β_2 and β_3 are the second-order and the third-order chromatic dispersion respectively. In order to compensate for the fiber loss, some EDFAs are added into the propagation links. It is assumed that the gains of the amplifiers are constant. $G = \exp(\alpha L_c)$, L_c is the length of fiber with attenuation α between two EDFAs. In order to suppress the amplified spontaneous emission (ASE) noise that EDFA brings, we select the optical band-pass filters which are Gaussion-like band-pass filters each with a 1.1-nm bandwidth. So the power of ASE is $P_{\rm ASE} = 2n_{\rm sp}(G-1)\cdot h\upsilon\cdot\Delta f$, where $n_{\rm sp}$ is the spontaneous emission factor.

3. Result and discussion

The parameters used in our numerical evaluation are listed in Table 1. By using the Simulink tools provided by MATLAB, the model of communication system in Eqs. (4)–(7) can be established. The differential equations are solved according to the principle of four-order Runge–Kutta.

Table 1. Simulation parameters.

Symbol	Description	Units
ω_0	Laser oscillation frequency	1.216×10^{15} s^{-1}
g	Gain coefficient	1.5×10^{-8} ps^{-1}
s	Gain saturation coefficient	5×10^{-7}
α	Linewidth enhancement factor	5
$\beta_{\rm sp}$	Spontaneous emission factor	1.5×10^{-9} ps^{-1}
e	Electron charge	1.602×10^{-19} C
N_0	Carrier number at transparency	1.5×10^{8}
$\tau_{n_{\rm t,r}}$	Carrier lifetime	2 ns
$\tau_{p_{\rm t,r}}$	Photon lifetime	2 ps
T	External cavity roundtrip time	0.2 ns
γ	Feedback coefficient	0.01, 0.02 ps^{-1}
$k_{\rm inj}$	Injection parameter	0.2, 0.15 ps^{-1}
$n_{\rm sp}$	Spontaneous emission factor	1.5

The power of an optical wave generated by TL and injected into the fiber is calculated by $P_{\rm t}(t) = (h\omega_0 c\alpha_m)/(4\pi\mu_{\rm g})\cdot|E_{\rm t}(t)|^2$, where h is the Planck constant, c is the velocity of light, α_m is the loss at the head face of fiber, and $\mu_{\rm g}$ is the group index. Here, $\alpha_m = 46$ cm^{-1} and $\mu_{\rm g} = 4$. Two types of fiber segments, SMF and DCF, are employed in our simulation (see Table 2).

Table 2. Fiber parameters.

Type	Parameters			
	β_2/(ps^2/km)	β_3/(ps^3/km)	γ/(W^{-1}/km)	α/(dB/km)
SMF	–21	0.1	1.06	0.21
DCF	190.1	0.1	5.07	0.549

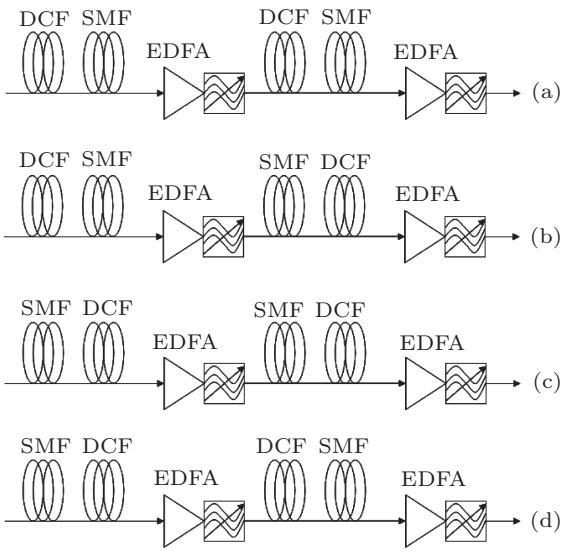


Fig. 2. Schematic diagram of dispersion compensation in the fiber link, showing (a) the pre-compensation map, (b) the symmetrical map (type I), (c) post-compensation map, and (d) symmetrical map (type II).

Four types of dispensation compensation maps for fiber link are considered. Figure 2 shows a period of each map. The unique difference among all maps is that the segments of compensation fiber (DCF) are located at different places. The period length is the same for each map, and two EDFAs are used in the middle and at the end of a period to compensate for the total losses occurring in the previous fiber spans. By choosing the segments of SMF and DCF each with an appropriate length, the total dispersion along the whole transmission period is set to be zero.

For the following simulation, a message of 1-Gb/s bit rate is hidden in the transmitter laser by the encryption method of CM or CSK. The modulation depth is set to be 5% to hide the information well into the chaotic carrier generated by the TL. The driving currents of transmitter and receiver are both set to be 23 mA, the feedback parameter of the transmitter is $\gamma = 0.01$ ps^{-1}, and the injection parameter of the receiver is $k_{\rm inj} = 0.2$ ps^{-1} to achieve the strong injection condition. The relationship between mean optical power injected into the fiber links and the corresponding Q factor for one transmission period, 100 km, is presented in Fig. 3.

It is obvious that the Q factor first increases and then decreases with the increase of injected optical power. This is the joint influence of nonlinear effect and ASE noise induced by EDFAs in fiber link. At a small injected optical power, the strength of signal is smaller than that of ASE noise which is constant for the same gain of EDFAs. At a large injected optical power, the SPM induced by nonlinear effect in fiber increases. The two cases degrade the quality of decoded message, which is indicated by small Q factor. The max Q factor will be attained at an appropriate optical power.

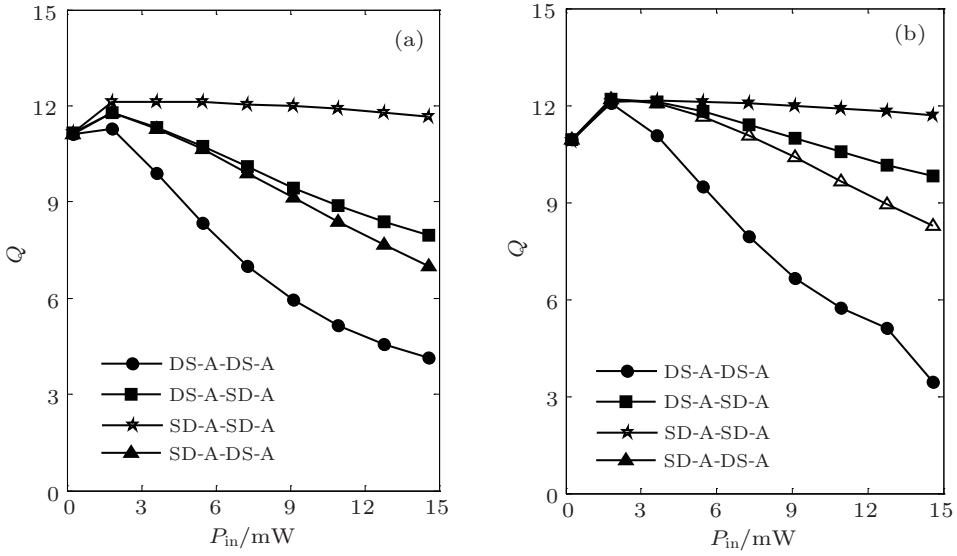


Fig. 3. Curves for Q factor for 1-Gb/s and 5% modulation depth versus mean optical power injected into fiber, obtained by (a) CM method and (b) CSK method.

According to an optimal power extracted from Fig. 3, the performance of the communication system with respect to transmission distance is investigated. The result is presented in Fig. 4. Here, 100-km and 200-km-length periods are considered. Remote communication can be realized by utilizing multiple periods. It indicates that the scheme of dispersion compensation has little effect on the quality of recovered information when the distance is smaller than 100 km, and the Q factor is kept at a high level (about 12). However, with the increase of transmission distance, the Q factor decreases at a different speed when each map is employed. For the CM method [Fig. 4(a)] and CSK method [Fig. 4(b)], in the case of 100-km-period, the Q factor decreases rapidly with the increase of transmission distance when the pre-compensation map is employed, however it decreases slowly when the post-compensation map is employed. The Q factor reaches 10 at 600 km for the latter map. The performances of the other symmetrical maps are almost the same, and they are between the performance of pre-compensation map and that of post-compensation. The result is accordant with that in Ref. [2], where the symmetrical map is proved to be better than pre-compensation map. However, in our experiment, the post-compensation map is indicated

to be better than symmetrical map, and is the best map for remote communication. In pre-compensation map, the DCF with strong nonlinear effect follows directly the EDFA, and the strong optical power in DCF leads to seriously self-phase modulation (SPM). The cumulated nonlinear effect deteriorates the quality of recovered information as distance increases. In the post-compensation, the DCF is far from the former EDFA, the optical power is attenuated after the former SMF segment, thus, the quality of recovered information is deteriorated slowly. In the two kinds of symmetrical maps, the mean distances between DCF segment and its former EDFA are similar.

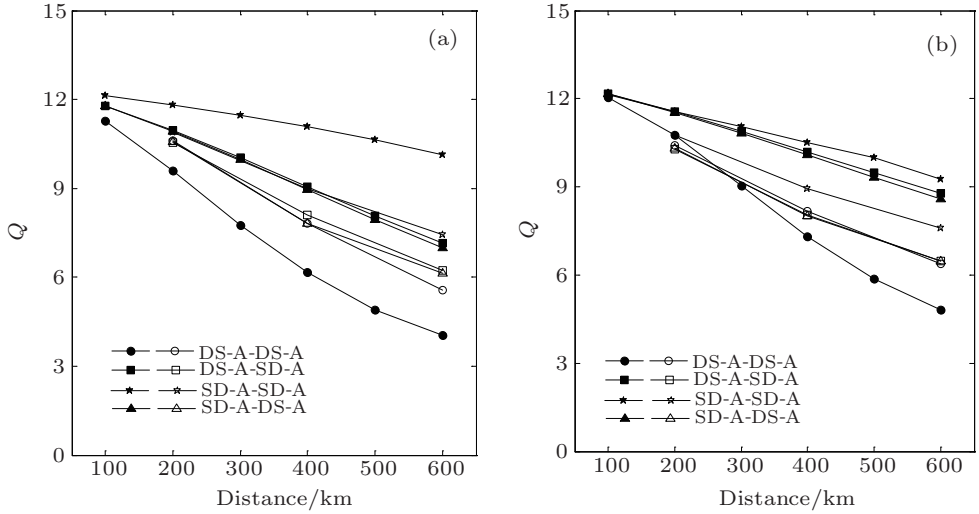


Fig. 4. Curves for Q factor for 1 Gb/s and 5% modulation depth versus transmission distance under the condition of 100-km period length (solid symbols) and 200-km period length (blank with cross symbols), obtained by the (a) CM method and (b) CSK method, respectively.

The cases of 200-km-length period in Fig. 4(a) and Fig. 4(b) show that the performance of pre-compensation map increases, but the performances of the other maps decrease. This is because that the nonlinear effect is dominant in the pre-compensation map. The mean distance between DCF and its former EDFA increases as the length of a period increases, thereby leading the decoding quality to ameliorate. However, nonlinear effect is small and the ASE noise is dominant in the other maps. When the period is lengthened, the increased ASE noise will worsen the decoding quality. At the same time, it is noticed that the post-compensation remains best. The result is shown in Fig. 5. A comparison of Fig. 5 with Fig. 4 indicates that the decoding quality is deteriorated seriously. It is because the spectrum of information is near to that of chaotic carrier. A lot of high-frequency spectra in chaotic carrier remain after filtering. Comparing the performances of the four maps in Fig. 5, we can find that the post-compensation map just keeps slight superiority for the 2.5-Gb/s message. In addition, the bigger Q factor in Fig. 5(a) than that in Fig. 5(b) indicates that the CM method benefits the application of high-speed communication.

In order to improve the recovering quality of the encrypted message, it is necessary to change the parameters of the system. The driving currents both in transmitter and receiver laser are set to be 40 mA, the feedback coefficient in transmitter laser is set to be 0.02 ps^{-1}, and the injection coefficient in receiver laser is set to be 0.15 ps^{-1}. By using these modifying parameters, the security of the system is still maintained at a high level. The result is presented in Fig. 6.

In Fig. 6, the performances of the two symmetrical compensation maps are the same, and they are better than those of the pre-compensation and pre-compensation maps. A comparison between the Q factor curves of post-compensation map in Fig. 5(a) and those of the symmetrical compensation map in Fig. 6(a) shows that the decoding quality is improved apparently, thus appropriately setting the values of parameters of system is necessary for the high-speed communication. Besides, the symmetrical compensation map is the best scheme for the recovery of a message encrypted by the CM method. In addition, it is noticed that the Q factor for the CSK method also increases after the appropriate parameters are used. However, the performance of the symmetrical compensation map is always close to that of the post-compensation map.

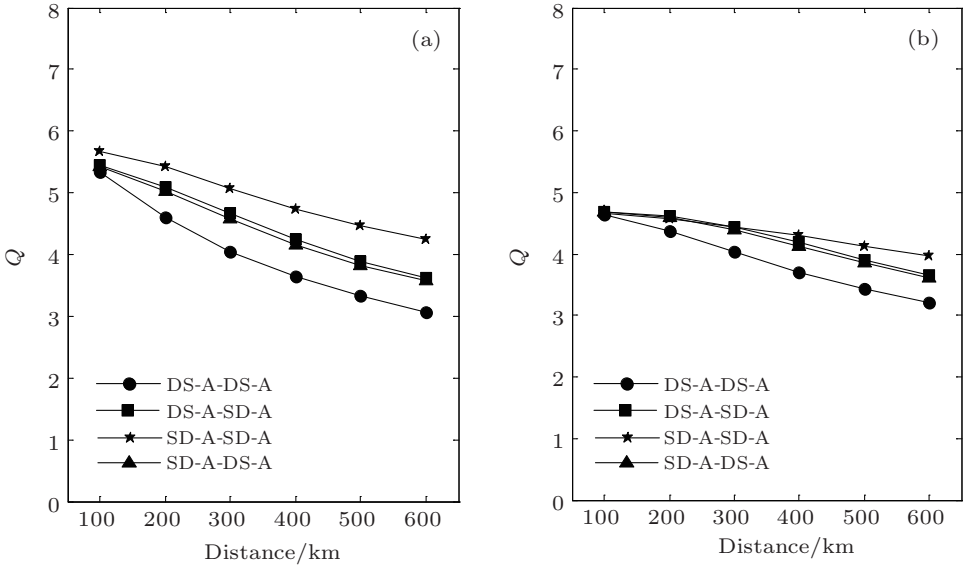


Fig. 5. Curves for Q factor for 2.5-Gb/s and 5% modulation depth versus transmission distance under the condition of 100-km period, $I = 23$ mA, $\gamma = 0.01$ ps^{-1}, and $k_{\rm inj} = 0.20$ ps^{-1}, obtained by the (a) CM method and (b) CSK method, respectively.

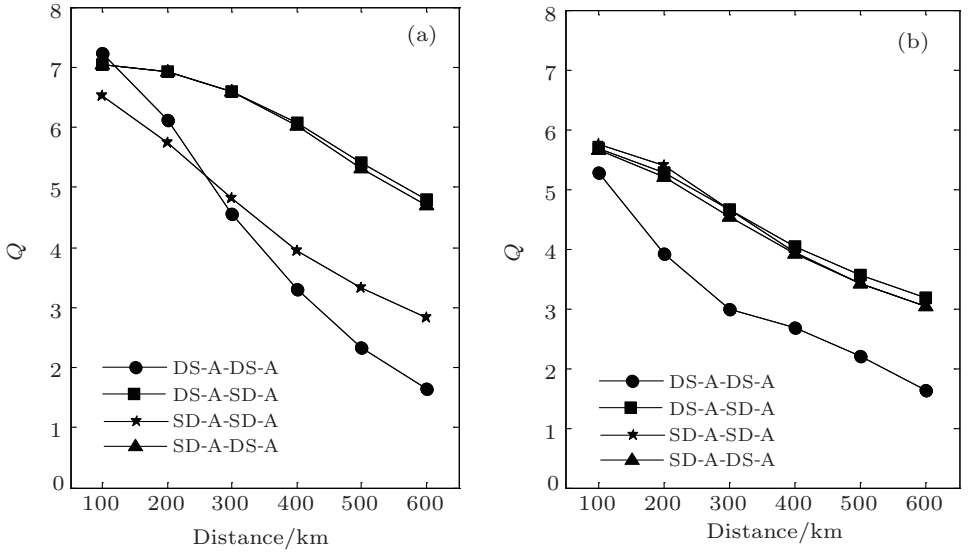


Fig. 6. Curves for Q factor for 2.5-Gb/s and 5% modulation depth versus transmission distance under the condition of 100-km period, $I = 40$ mA, $\gamma = 0.02$ ps^{-1}, and $k_{\rm inj} = 0.15$ ps^{-1}, obtained by the (a) CM method and (b) CSK method.

4. Conclusion

The numerical investigation of an optical chaotic communication system with open-loop configuration using fiber transmission is performed. The performance comparison among four compensation maps is demonstrated by means of Q factor calculation. Two kinds of bit rates of messages and two encryption methods are utilized. The experimental result indicates that the performance of a pre-compensation map is always worst, and two types of symmetrical maps are identical, no matter which encryption method is used and what the bit rate of the message is. For a lower bit rate message, the post-compensation map is the best scheme. It is still better than the other three maps even if the transmission period increases. For a higher bit rate message, it is necessary to modify the parameters in the communication system to change the spectrum of the chaotic carrier of the transmitter. For high-speed application, the CM method is superior to the CSK method for the recovery of the message, and this result is accordant with that in the case of back-to-back configuration. Two types of symmetrical maps are the best scheme. However, for the CSK

method, there is no apparent difference between the performances of the symmetrical compensation map and the post-compensation map.

References

[1] Liu H J and Feng J C 2009 *Acta Phys. Sin.* **58** 1484 (in Chinese)

[2] Kanakidis D, Argyris A and Syvridis D 2003 *IEEE Lightwave Technology* **21** 750

[3] Kanakidis D, Bogris A, Argyris A and Syvridis D 2004 *IEEE Lightwave Technology* **22** 2256

[4] Argyris A and Kanakidis D 2005 *IEEE Quantum Electronics* **41** 892

[5] Yan S L 2006 *Acta Phys. Sin.* **55** 6267 (in Chinese)

[6] Wu J G, Wu Z M and Lin X D 2005 *Acta Phys. Sin* **54** 4170 (in Chinese)

[7] Y S L, Chi Z Y and Chen W J 2004 *Chin. J. Ins. Commun.* **25** 78 (in Chinese)

[8] Wu L and Zhu S Q 2003 *Chin. Phys.* **12** 300

[9] Wu L and Zhu S Q 2003 *Phys. Lett.* A **308** 157

[10] Wu L and Zhu S Q 2004 *Commun. Theor. Phys.* **41** 225

[11] Sugawara T, Tachikawa M, Tsukamoto T and Shimizu T 1994 *Phys. Rev. Lett.* **72** 3502

[12] Tang L M, Dykstra R and Heckenberg N R 1996 *Phys. Rev. Lett.* **54** 5317

[13] Yan S L 2005 *Chin. J. Lasers* **32** 1503 (in Chinese)

[14] Li X F, Pan W, Luo B and Ma D 2006 *IEEE Quantum Electronics* **42** 953

[15] Kanakidis D and Argyris A 2006 *IEEE Lightwave Technology* **24** 335

[16] Argyris A, Kanakidis D, Bogris A and Syvridis D 2004 *IEEE Quantum Electronics* **10** 927

[17] Yan S L 2005 *Elec. Sin.* **33** 266 (in Chinese)

[18] Yan S L 2005 *Acta Phys. Sin.* **54** 2000 (in Chinese)

[19] Argyris A and Syvridis D 2004 *IEEE Lightwave Technology* **22** 1272

[20] Argyris A, Kanakidis D and Dimitris S 2003 *Proc. Optical Fiber Communication Conference* (Atlanta, USA)

[21] Paul J, Lee M W and Shore K A 2005 *IEEE Photonics Technology Lett.* **17** 920

[22] Valerio A L, Mauro B, Sabina M, Michele N and Biagio P 2005 *IEEE Photonics Technology Lett.* **17** 1995

[23] Kouomou Y C, Colet P, Larger L and Gastaud N 2005 *IEEE Quantum Electronics* **41** 156